JPn Neuroscience

The Journal of Physiology

J Physiol 590.10 (2012) pp 2285–2304

Neurons respond directly to mechanical deformation with pannexin-mediated ATP release and autostimulation of $P2X_7$ receptors

Jingsheng Xia[1], Jason C. Lim[1], Wennan Lu[1], Jonathan M. Beckel[1], Edward J. Macarak[1], Alan M. Laties[2] and Claire H. Mitchell[1,3]

Departments of [1]Anatomy & Cell Biology, [2]Ophthalmology and [3]Physiology, University of Pennsylvania, Philadelphia, PA 19104, USA

Key points

- Neurons can be damaged when tissues are stretched or swollen; while astrocytes can contribute to this process, the mechanosensitive response from neurons is unclear.
- We show here that isolated retinal ganglion cell neurons respond to mechanical strain with a rapid, sustained release of the neurotransmitter ATP.
- The conduit for ATP release was through pannexin hemichannels, with probenicid, carbenoxelone and ^{10}panx inhibiting release.
- Once released, this ATP acts back on the neurons to autostimulate lethal $P2X_7$ receptors, as A438079, AZ 10606120 and zinc reduced currents in whole cell patch clamp recordings.
- Blocking release of ATP through pannexin channels, or activation of $P2X_7$ receptors, might be neuroprotective for stretched or swollen neurons.
- Stretch-dependent release of ATP through neuronal pannexins, combined with the autostimulation of the $P2X_7$ receptors, provides a new pathway by which neuronal activity and health can be altered by mechanical strain independently of glial activity.

Abstract Mechanical deformation produces complex effects on neuronal systems, some of which can lead to dysfunction and neuronal death. While astrocytes are known to respond to mechanical forces, it is not clear whether neurons can also respond directly. We examined mechanosensitive ATP release and the physiological response to this release in isolated retinal ganglion cells. Purified ganglion cells released ATP upon swelling. Release was blocked by carbenoxolone, probenecid or peptide ^{10}panx, implicating pannexin channels as conduits. Mechanical stretch of retinal ganglion cells also triggered a pannexin-dependent ATP release. Whole cell patch clamp recording demonstrated that mild swelling induced the activation of an Ohmic cation current with linear kinetics. The current was inhibited by removal of extracellular ATP with apyrase, by inhibition of the $P2X_7$ receptor with A438079, zinc, or AZ 10606120, and by pannexin blockers carbenoxolone and probenecid. Probenecid also inhibited the regulatory volume decrease observed after swelling isolated neurons. Together, these observations indicate mechanical strain triggers ATP release directly from retinal ganglion cells and that this released ATP autostimulates $P2X_7$ receptors. Since extracellular ATP levels in the retina increase with elevated intraocular pressure, and stimulation of $P2X_7$ receptors on retinal ganglion cells can be lethal, this autocrine response may impact ganglion cells in glaucoma. It remains to be determined whether the autocrine stimulation of

J. Xia and J. C. Lim contributed equally to this work.

DOI: 10.1113/jphysiol.2012.227983

purinergic receptors is a general response to a mechanical deformation in neurons, or whether preventing ATP release through pannexin channels and blocking activation of the $P2X_7$ receptor, is neuroprotective for stretched neurons.

(Resubmitted 11 January 2012; accepted after revision 6 March 2012; first published online 12 March 2012)
Corresponding author C. H. Mitchell: Department of Anatomy and Cell Biology, University of Pennsylvania, 440 Levy Building, 240 S. 40th St, Philadelphia, PA 19104, USA. Email: chm@exchange.upenn.edu

Abbreviations LDH, lactate dehydrogenase; PD, postnatal day; RGC, retinal ganglion cell; RVD, regulatory volume decrease.

Introduction

Mechanical deformation frequently leads to neuronal damage. Stretching neurons in a model of traumatic brain injury leads to apoptosis (Lau *et al.* 2006). Elevated intracranial pressure can accompany encephalitis, with the clinical outcome proportional to the elevation (Treggiari *et al.* 2007; Kumar *et al.* 2009). Similarly, increased intraocular pressure (IOP) produces complex mechanical deformations that may contribute to glaucomatous optic neuropathy (Sigal & Ethier, 2009). While the generalized cascades culminating in neuronal death have been intensively studied (Lossi & Merighi, 2003), less is known about the initial steps linking mechanical strain to neuronal damage, even though these early mechanisms could provide key therapeutic targets for reducing the neuronal loss that accompanies mechanical strain.

The physiological release of ATP is used throughout the body to transduce mechanical signals into chemical ones. Increased sheer stress (Burnstock, 1999, Woo *et al.* 2008), stretching (Sadananda *et al.* 2009), and swelling (Boudreault & Grygorczyk, 2004) of tissues all trigger a physiological ATP release. Moreover, the stretch accompanying inhalation may initiate ATP release in bronchial epithelial cells (Winters *et al.* 2007), while bladder distention also triggers ATP release (Ferguson *et al.* 1997). Increasing evidence implicates the mechanosensitive release of ATP in the nervous system too, with most reports identifying astrocytes as the cellular source. Astrocytes release ATP when mechanically prodded (Newman, 2001, 2003; Zhang *et al.* 2008), swollen (Darby *et al.* 2003) or subjected to shear stress (Shitta-Bey & Neary, 1998; Neary *et al.* 2005). While astrocytes possess the mechanisms to release ATP through both vesicular and non-vesicular pathways, the release triggered by mechanical deformation may utilize non-vesicular routes (Joseph *et al.* 2003). ATP released by astrocytes can diffuse through extracellular space to influence neuronal activity (Pascual *et al.* 2005; Halassa *et al.* 2009). This ATP can stimulate P2 receptors for ATP, but the abundance of ectonucleotidases and ectonucleosidases usually converts this extracellular ATP into adenosine, with preferential stimulation of neuronal adenosine receptors (Newman, 2003).

While mechanosensitive release of ATP from astrocytes is undoubtedly important, the enthusiasm accompanying the glial revolution may have overshadowed potential contributions from neurons. Classic vesicular release of ATP from the synaptic regions of neurons is well established (Gonzalez-Sistal *et al.* 2007), but release through non-vesicular conduits has not been thoroughly studied. However, several observations suggest retinal ganglion cells are capable of mechanosensitive ATP release through non-vesicular pathways. For example, mild elevation of pressure across the retina triggers a release of ATP that is inhibited by blockers of pannexin-1 hemichannels (Reigada *et al.* 2008). Pannexin-1 provides a conduit for mechanosensitive ATP efflux (Bao *et al.* 2004), and the retinal expression of pannexin-1 is highest in ganglion cells (Dvoriantchikova *et al.* 2006). These observations all suggest that ganglion cells could be a source of mechanosensitive ATP release. On this basis, the neuronal contribution to mechanically sensitive ATP release from retinal ganglion cells was examined, with the conduit for release and the physiological consequences of this release also investigated.

Portions of this work have been previously presented in abstract form (Lim *et al.* 2010, Mitchell *et al.* 2010, Mitchell *et al.* 2010a; Xia *et al.* 2010).

Methods

Animals

All procedures were carried out according to the guidelines laid down by the University of Pennsylvania IACUC board using procedures approved by the board. These conform to the principles of UK regulations, as described in Drummond (2009). Animals were obtained from Harlan Laboratories.

Preparation of mixed retinal cell suspension

Pups from untimed pregnant Long–Evans rats (Harlan Laboratories, Indianapolis, IN, USA) were killed on postnatal day (PD) 3–10, with pups anaesthetized by an intraperitoneal injection of 50/5 mg kg^{-1} ketamine/xylazine followed by cervical dislocation. The retinas were

dissected in Hanks' balanced salt solution (HBSS; Gibco/Invitrogen Corp., Carlsbad, CA, USA). The tissue was dissociated enzymatically by incubation with 15 U ml^{-1} papain (Worthington, Lakewood, NJ, USA) and 0.2 mg ml^{-1} DL-cysteine in HBSS for 15 min at 37°C. Retinas were washed with HBSS and triturated 50 times to dissociate the cells. For investigating the ATP release stimulated by cell swelling, cells were centrifuged, re-suspended in isotonic solution (containing, in mM: 105 NaCl, 5 KCl, 4 Na-Hepes, 6 Hepes acid, 5 $NaHCO_3$, 60 mannitol, 5 glucose, 1.3 $CaCl_2$ and 0.5 $MgCl_2$; pH 7.4), and plated on a 96-well white plate. For cell stretch experiments, the cells were seeded on a silicone sheet coated with 0.05% poly-L-lysine and 10 μg ml^{-1} laminin (BD Biosciences, Bedford, MA, USA) in a specially designed stretch chamber (see below) and maintained at 37°C with 5% CO_2. The basic growth medium contained Neurobasal medium with 0.033 ml ml^{-1} B27 supplement, 2 mM glutamine, 50 μg ml^{-1} gentamicin (all Invitrogen Corp.), 3.3% rat serum (Cocalico Biologicals Inc., Reamstown, PA, USA) and 0.7% methylcellulose (Stemcell Technologies Inc., Vancouver, BC, Canada). For patch clamp experiments, ganglion cells were first back-labelled by the injection of aminostilbamidine or 1,1′-dioctadecyl-3,3,3′,3′-tetramethylindocarbocyanine perchlorate ($DiIC_{18}$; Invitrogen Corp.) into the superior colliculus. Rats were anaesthetized with an intraperitoneal injection of 50/5 mg kg^{-1} ketamine/xylazine and the dye injected as described (Zhang *et al.* 2005). After allowing 2–3 days for the transport of the dye to the retina, animals were killed as above, and retinal cells were prepared as above and plated onto coverslips coated with poly-L-lysine and laminin. Ganglion cells were identified by the fluorescent label.

Measurement of ATP

ATP levels were determined using the chemiluminescent luciferin–luciferase reaction using a microplate luminometer (Luminoskan Ascent; Labsystems, Franklin, MA, USA). The luciferin–luciferase assay mix was prepared in a stock solution using one vial of the ATP assay mix (FLAA, Sigma-Aldrich Co.) diluted in 450 μl of isotonic solution and 50 μl of distilled water. The working solution was prepared by diluting 100 μl of the stock solution in 1 ml of isotonic solution. To determine ATP levels, 5 μl of cell suspension was incubated in 5 μl of isotonic control or isotonic solution with either 5 μl of carbenoxolone (10 μM; 30 min preincubation) or 5 μl of probenecid (1 mM; 15 min preincubation). After preincubation, 5 μl of luciferin–luciferase working solution was added and the cells were distributed into a 96-well white plate. Eighty-five microlitres of isotonic solution (295 mosmol l^{-1}), hypotonic solution (made by the addition of 25–35% H_2O, 214–186 mosmol l^{-1}, respectively), hypotonic solution including pannexin-1 channel blockers, or isotonic solution with 60 mM mannitol removed (228 mosmol l^{-1}) was added from a template using a multi-channel pipettor to wells and emitted light was measured using the luminometer. Analysis of ATP released during stretch experiments was performed by adding 30 μl luciferase mixture to 20 μl extracellular solution with 50 μl of isotonic solution per well of a white 96-well plate. The light from each well was recorded every 13 s for 20 min, with an integration time of 100 ms per measurement. Luminescence values were converted to ATP concentration using an ATP standard curve prepared daily. Correction for the minor effect of drugs on the luciferase assay was performed.

It should be noted that care was taken to try to standardize cell number as much as possible within each trial. Cells were counted with a hemocytometer and cells were diluted by the correct amount to ensure all experiments were performed using the same concentration of cells. The vial with the cell suspension was inverted regularly to prevent settling, while cells were plated in the precise order from the suspension vial to ensure that control and experimental wells experienced roughly the same degree of settling. In spite of these precautions, variation did occur. As such, levels were normalized to the mean control levels for each day's experiments. Although the restricted number of immunopanned cells, as compared to mixed cells, meant the cell numbers were different, these precautions ensured comparisons could be made between different treatments of the same preparations.

Cell stretch chamber

A custom designed stretch chamber was used to investigate the ATP release triggered by cell stretching (Winston *et al.* 1989). Small cylinders whose bottoms were lined with an elastic silicone material (Silastic, Speciality Manufacturing, Saginaw, MI, USA) were used. Silicone sheets were coated with poly-L-lysine for 24 h and laminin for 2 h prior to seeding. Either mixed retinal cells or isolated retinal ganglion cells (RGCs) were seeded onto the silicone sheets in the stretch chamber and maintained in growth medium at 37°C for 24 h in a humidified atmosphere of 5% CO_2 in air. After carefully washing the cells with isotonic solution, 700 μl of either control or experimental solution was added. After 30 min rest, a 50 μl aliquot of extracellular solution was obtained from the centre of the chamber approximately 1 mM above the cells as a baseline sample. The silicone substrate and the attached cells were deflected downward following injection of air into the upper compartment of the chamber. The pressure in the upper compartment

was quantified using a digital manometer (World Precision Instruments Inc., Sarasota, FL, USA). Pressure in the upper compartment of the stretch chamber was increased to 20 mmHg and returned to 0 mmHg every 30 s over a period of 2 min. Application of 20 mmHg of pressure was calculated to induce a 4.1% strain in the membrane as determined by measuring its downward linear displacement from the horizontal plane using the formula $\varepsilon = 0.66(\omega_0/a)^2$ where ω_0 is the peak downward deflection and a the radius of the substrate (Winston *et al.* 1989). Immediately following this stretch protocol, a 50 μl sample of the extracellular solution was collected as above. ATP concentrations were determined using the luciferin–luciferase assay.

Lactate dehydrogenase assay

Lactate dehydrogenase (LDH) released into the extracellular solution was measured as an indicator of cell membrane integrity, based on a coupled two-step reaction where tetrazolium salt was reduced to the coloured product formazan by enzyme activity (Cytotoxicity Detection Kit LDH, Roche Applied Science). Briefly, cells were incubated in 100 μl of either isotonic or hypotonic solution for 20 min in a 96-well plate, or 100 μl of extracellular solution collected from cells subject to stretch was added to a 96-well plate. A reaction mixture consisting of catalyst and dye solution was prepared and 100 μl was added to each well as per the manufacturer's instructions. After incubation for 15–30 min at room temperature, the dye absorbance was measured at 490 nm using a microplate reader. Absorbance values were converted to LDH concentration by preparing LDH standards (L-LDH; from rabbit muscle, Roche) for each experiment. The hypotonic solution did not affect the LDH assay.

RGC purification

RGCs were isolated using the immunopanning procedure of Barres *et al*. (1988) as described previously (Zhang *et al.* 2006). Briefly, neonatal rat retinas were dissociated with papain. Cells were incubated with rabbit antimacrophage antibody (1:75, Accurate Chemical, Westbury, NY, USA), then incubated in a 100 mm dish coated with goat anti-rabbit IgG antibody (1:400, Jackson ImmunoResearch Laboratories Inc., West Grove, PA, USA). Non-adherent cells were removed to a second petri-dish coated with goat anti-mouse IgM (1:300, Jackson ImmunoResearch Laboratories) and anti-Thy 1.1 antibody (from hybridoma T11D7e2; American Type Culture Collection, Rockville, MD, USA). After 30 min, non-adherent cells were washed off and the remaining cells were incubated with 0.125% trypsin for 8 min at 37°C. Digestion was stopped with fetal bovine serum (30%) in Neurobasal medium, and cells were centrifuged and either plated on relevant substrate or used immediately for ATP release measurements.

Patch clamping recordings

To determine whether mechanically sensitive ATP release was capable of stimulating ionic currents, RGCs were swollen by exposure to hypotonic solution and the whole cell currents evoked by cell swelling were characterized based on approaches used previously (Mitchell *et al.* 1997, 2002). The resistance of pipettes was 3–6 MΩ when filled with pipette solution (in mM): 140 CsCl, 10 tetraethylammonium-Cl, 10 Hepes, 5 EGTA, 2 MgATP, 2.67 $CaCl_2$, pH 7.3 (free $[Ca^{2+}] = 80$ nM, EGTA Calculator; http://brneurosci.org/cgi-bin/egta.html). The isotonic bath solution contained (in mM): 105 NaCl, 10 tetraethylammonium-Cl; 10 Hepes, 2 $CaCl_2$, 5 glucose, 75 mannitol (pH 7.4). Swelling cells by the addition of 30% water frequently led to a loss of seal; presumably the large reservoir of intracellular solution effectively volume clamped the cell and prevented regulatory volume decrease normally enacted. Consequently, the solution was made hypotonic for patch clamp recordings by the removal of 30–75 mM mannitol. Cells were clamped for 100–200 ms each to voltages between −100 mV and −60 mV in 5 mV steps from a holding potential of −60 mV to avoid activation of voltage-dependent Na^+ currents. Once the evoked currents reached a plateau, drugs dissolved in hypotonic solution were added. Results from experiments performed using both bath addition and perfusion are combined as both approaches yielded similar results. Currents were recorded using two separate patch clamp systems. An Axopatch 200B amplifier was used with data analysed using pCLAMP 9.2 software (Axon Instruments) through an analog/digital interface (Digidata 1200, Axon Instruments). In addition, later experiments were performed using an EPC 10 amplifier with Patch Master analysis software (both HEKA Electronics Inc.). In both cases, signals were low-pass filtered at 1 kHz and sampled at 10 kHz.

RNA extraction, amplification and PCR

Total RNA was isolated from samples of total brain, spleen and retinal tissue, and immunopurified retinal ganglion cells from Long–Evans rats using Trizol Reagent (Invitrogen Corp.) and RNeasy spin columns (Qiagen Inc., Valencia, CA, USA), including an on-column DNase digestion step, in accordance with the manufacturer's protocol. RNA quantification was performed using a spectrophotometer (NanoDrop 2000, Thermo Scientific Inc.), and 260/280 ratios for all RNA samples were

between 2.00 and 2.08. Forty nanograms of isolated RNA was amplified using the WT-Ovation RNA Amplification System (NuGEN Technologies Inc., San Carlos, CA, USA) by strictly adhering to the manufacturer's instructions and negative reverse transcriptase controls were run by omitting the First Strand Enzyme Mix from reactions. Amplified cDNA was diluted 1:5 and 2 μl of cDNA template was used for PCR amplification with 200 nM (panx1) or 300 nM ($P2X_7$) of each forward and reverse primer and 2.5 units of Taq DNA polymerase (Invitrogen Corp.). The primer sequences were as follows: pannexin-1 – forward 5′-GCTGTGGGCCATTATGTCTT-3′ and reverse 5′-GCAGCCAGAGAATGGACTTC-3′ yielding a 234 bp amplicon; $P2X_7$ – forward 5′-GGAAGATCCGGAAG GAGTTC-3′ and reverse 5′-GACATGGACGGGAGAGA AAA-3′ yielding a 392 bp amplicon. PCR reactions (50 μl) were carried out on a Veriti 96-well Thermal Cycler (Applied Biosystems, Foster City, CA, USA) using the following thermal cycle profile – initial denaturation at 95°C for 2 min, 40 cycles of denaturation (95°C for 15 s), annealing (57°C or 60°C for $P2X_7$ or pannexin-1, respectively, for 30 s) and extension (72°C for 30 s), followed by a final extension at 72°C for 10 min. The PCR products were analysed by electrophoresis separation on a 1.5% agarose gel and visualized by ethidium bromide staining. PCR products were sequenced at the University of Pennsylvania sequencing facility.

Immunohistochemistry

Retinal ganglion cells were purified using a two-step immunopanning procedure as described. Cells were plated on 25 mm glass coverslips coated with 0.05% poly-L-lysine (Peptides International Inc., Louisville, KY, USA) and 1 μg ml^{-1} laminin (from mouse, BD Biosciences) and maintained with Neurobasal media supplemented with B27 (Invitrogen), forskolin (10 μM; LC Labs, Woburn, MA, USA) and human brain-derived neurotrophic factor (25 ng ml^{-1}; Peprotech, Rocky Hill, NJ, USA) for 48 h. The medium was then removed and the cells fixed using 4% paraformaldehyde in 0.1 M phosphate buffered saline (PBS) for 30 min. After washing with PBS, the cells were permeablized using 0.1% Triton X-100 and blocked using 10% donkey serum (Millipore). The coverslips were then incubated in their primary antibodies diluted in 1% donkey serum overnight at 4°C. The primary antibodies (and concentrations) used were: (1) rabbit anti-$P2X_7$ (Alomone Labs Ltd, Jerusalem, Israel; 1:100 dilution) and goat anti-pannexin-1 (Santa Cruz Biotechnology, Inc., Santa Cruz, CA, USA, 1:100 dilution). The following day the coverslips were washed with PBS and incubated in secondary antibodies (donkey anti-goat FITC and donkey anti-rabbit rhodamine, 1:200 dilution each) for 2 h. Following a wash, the cells were also stained with DAPI (300 nM, 2 min incubation) as a nuclear counter stain. Coverslips were mounted onto glass slides using Slowfade Gold anti-fade mounting medium (Invitrogen). Results were observed using a Nikon A1R confocal microscope using a 100× objective (CFI Plan Apo VC 100× Oil, NA 1.40) and the NIS-Elements C software package. The micrograph consisted of images taken of four adjacent fields of view observed with a 100× oil immersion objective and combined digitally.

Regulatory volume decrease

Regulatory volume decrease was determined based on an approached used previously (Mitchell *et al.* 2002). Briefly, isolated RGCs were plated on coverslips and allowed to attach for 24 h. Cells were loaded with 4 μM calcein-AM and 0.02% Pluronic at room temperature for 40 min, followed by a gentle wash. Cells were imaged with an inverted microscope equipped for fluorescence (Nikon Diaphot, Nikon USA). Cells were imaged every 20 s, with fluorescence excited at 488 nM and emitted >520 nm recorded with a camera and processed (all Photon Technologies International, Inc., Lawrenceville, NJ, USA). Cells were perfused at room temperature with control solution containing (in mM): 105 NaCl, 5 KCl, 4 Na-Hepes, 6 Hepes acid, 1.3 $CaCl_2$, 5 glucose, 5 $NaHCO_3$, 60 mannitol, pH 7.4, 295 mosmol l^{-1}; the solution was made hypotonic by the addition of 30% H_2O, 200 mosmol l^{-1}. To determine cell area, images were thresholded to remove background fluorescence and cell area was defined as the number of non-black pixels after thresholding. The area values were converted to volume using standard equations, assuming the image represented the maximal cross sectional area. Regulatory volume decrease was defined as $100 \times (H - H_{30})/(H - I)$, where H is peak cell volume in hypotonic solution, H_{30} is volume after 30 min in hypotonic solution and I is volume in isotonic solution.

Materials

AZ 10606120, A438079, ^{10}panx and scrambled peptide were purchased from Tocris Bioscience (Ellisville, MO, USA). All other materials were from Sigma-Aldrich unless otherwise noted.

Data analysis

All data are expressed as means ± standard error of the mean. Significance was defined as $P < 0.05$ and was determined using a one-way ANOVA followed by Tukey's *post hoc* test using SigmaStat software (Systat Software, Inc., San Jose, CA, USA) unless otherwise noted. On

occasions when data were not normally distributed, ANOVAs were performed on ranks. To evaluate the effect of inhibitors, % Block = $100 \times ((S - S_B)/(S - C))$ where S is the response in swelling solution, S_B is the response in swelling solution + blocker, and C is the response in control. As absolute levels of ATP varied with the cell density of each preparation, levels were normalized to the mean ATP concentration in each day's experiments. Likewise, to overcome the large cell to cell variation in current size, currents were normalized to the peak current for each cell. For patch clamp experiments, n is cell number; for stretch experiments, n is the number of independent chambers used; for swelling experiments, n is the number of wells, with each trial repeated on >3 independent plates. To aid in the interpretation of results, the effect of blockers on ATP release from mixed cells are shown as grey with horizontal stripes while the effects on isolated ganglion cells are shown as grey with cross hatching.

Results

ATP release from swollen cells

Initial experiments examined the mechanosensitive release of ATP from cells swollen after exposure to hypotonic solution. This approach enabled an on-line readout of ATP levels to allow analysis of release kinetics. Addition of freshly dissociated mixed retinal cells to a hypotonic solution triggered a rapid release of ATP (Fig. 1*A*). In the mixed cells, ATP levels were maximal within 30 s of cell addition. Levels decreased at a steady rate after the initial peak, indicating the rate of ATP breakdown was greater than the release rate. Mean ATP levels over the initial 10 min were 12.9 ± 0.6-fold higher after hypotonic challenge (Fig. 1*B*). Of note, absolute ATP levels reflect the dilution of ATP released into a large extracellular volume; they are several orders of magnitude lower than levels expected near the cell membrane (Beigi *et al.* 1999).

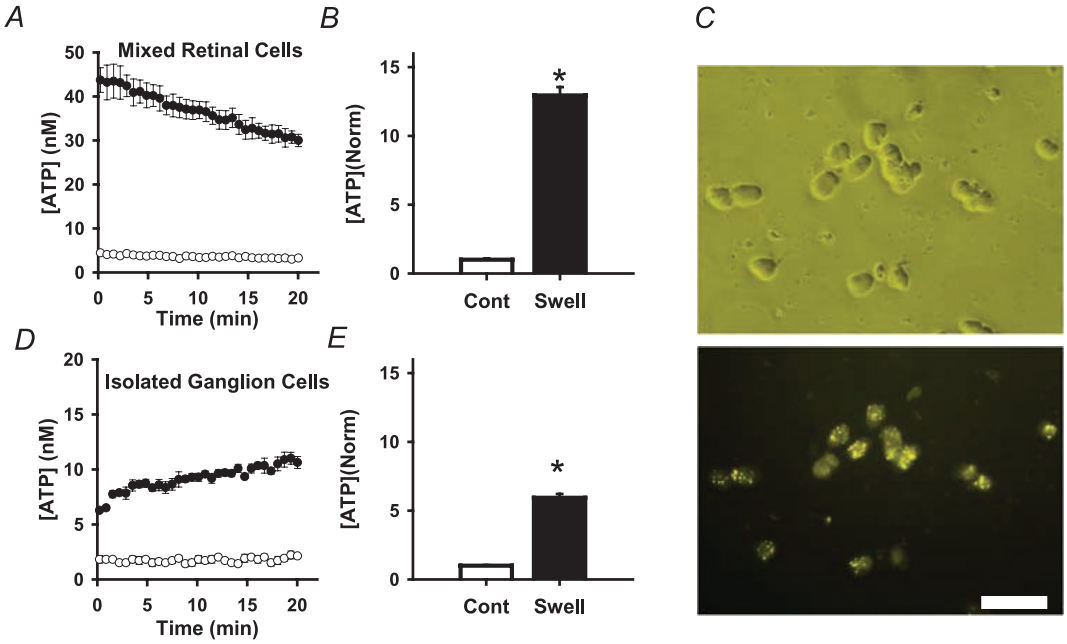

Figure 1. Cellswelling triggers the release of extracellular ATP from mixed retinal cells and isolated retinal ganglion cells
A, the kinetics of ATP release from mixed retinal cells exposed to control isotonic solution (open circles) and after swelling with a hypotonic solution prepared by diluting the isotonic solution with water (filled circles). Data represent means ± SEM from a representative experiment using 4 wells. *B*, mean levels of ATP in the extracellular solution rose significantly upon swelling with hypotonic solution. (n = 20 for control isotonic solution (Cont); n = 26 swollen in hypotonic solution (Swell), $^*P < 0.001$ *vs.* Control). Here and throughout, bar graphs depict the mean ± SEM levels normalized to the mean control levels of each day's experiments, using ATP levels obtained over the initial 10 min. *C*, fluorescently labelled immunopanned retinal ganglion cells shown in phase contrast (top) and excited at 360 nm (bottom). Label was detected in 95–98% of the isolated cells, confirming purity. Scale bar = 50 μm. *D*, typical curve showing the kinetics of ATP release from isolated retinal ganglion cells in control solution (open circles) or swollen in a hypotonic solution made by addition of water to the isotonic solution (filled circles). There was a rapid release of ATP over the initial 2.5 min, followed by a slower increase in ATP levels thereafter, suggesting a reduced activity of ectoATPases on ganglion cells as compared to mixed retinal cells. *E*, mean increase in extracellular ATP from purified isolated retinal ganglion cells swollen upon exposure to hypotonic solution. (n = 40 for each; $^*P < 0.001$ *vs.* Control).

To determine whether ATP release from the mixed retinal cell preparation reflected a contribution from retinal ganglion cells, these cells were isolated using the two-step immunopanning procedure. Purity of preparations was confirmed by labelling ganglion cells by injection of aminostilbamidine into the superior colliculus. After allowing 2–3 days for retrograde transport of the dye from the brain to the soma in the retina, ganglion cells were isolated. Typically 95–98% of isolated cells were labelled (Fig. 1*C*) confirming the purity of the preparation, as found previously (Zhang *et al.* 2006).

Purified isolated retinal ganglion cells also released ATP upon swelling (Fig. 1*D*). After the initial transient, ATP levels rose rapidly for the first 3 min, followed by a sustained increase at a slower rate, indicating the rate of release was greater than the rate of degradation. This suggests mixed retinal cells contain greater ectoATPase activity than isolated retinal ganglion cells, although other possibilities also exist. Overall, ATP levels in isolated ganglion cells were 5.9 ± 0.3-fold higher after swelling (Fig. 1*E*). While lower than the increase observed in mixed retinal cells, this may reflect the lower density of purified ganglion cells; panned cells had a density of 2375 ± 131 cells per well, while mixed cells were present at 6208 ± 63 cells per well. However, the precautions taken to control cell number within trials (see Methods) ensure that these comparisons between cells in like preparations are valid.

Several controls were performed to confirm that ATP release was physiologically relevant. First, the levels of lactate dehydrogenase (LDH) surrounding mixed retinal cells were not significantly altered by swelling cells for 20 min ($P = 0.48$, $n = 6$ for mixed cells). Likewise, 20 min of swelling did not increase levels of LDH surrounding isolated retinal ganglion cells ($P = 0.41$; $n = 4$). In contrast, lysis of the cells led to a large rise in LDH concentration. This implies that the increase in extracellular ATP surrounding either mixed retinal cells or isolated retinal ganglion cells was not due to non-specific rupture of the cell membrane. Secondly, swelling was also induced by the removal of 60 mM mannitol. This method of creating hypotonicity does not change the ionic strength of the solution bathing the cells, thus producing a more subtle hypotonic challenge. In mixed cells, the level of extracellular ATP rose from a normalized level of 1.0 ± 0.1 when in an isotonic solution with mannitol to 2.8 ± 0.2 upon mannitol removal ($P < 0.001$; $n = 20$–26). Likewise in isolated ganglion cells extracellular ATP levels rose from 1.0 ± 0.04 to 1.6 ± 0.1 ($P < 0.001$; $n = 38$–40). The magnitude of the ATP release is reduced with mannitol removal as compared to normal hypotonicity, consistent with smaller osmotic forces. However, the presence of a significant ATP release from both mixed retinal and isolated ganglion cell preparations implies that ATP release from swollen cells is mechanically based.

The contribution of pannexins to the swelling-activated release was examined by testing the ability of pannexin channel blockers to inhibit ATP release. Specific antagonists for the pannexin channel do not currently exist, but the channel can be identified using a combination of antagonists at concentrations where these drugs are somewhat selective (Silverman *et al.* 2008; Bruzzone *et al.* 2005). Carbenoxolone (10 μM) and probenecid (1 mM) reduced the level of ATP released into the bath from both mixed retinal cells and purified ganglion cells (Fig. 2*A* and *D*). The ATP levels surrounding mixed retinal cells after swelling were reduced $43.5 \pm 3.6\%$ by carbenoxolone and $55.2 \pm 3.7\%$ by probenecid (Fig. 2*B* and *C*). The ATP release from swelling purified ganglion cells was reduced $44.0 \pm 3.0\%$ by carbenoxolone and $45.5 \pm 6.5\%$ by probenecid (Fig. 2*E* and *F*). The ability of both compounds to inhibit ATP release is consistent with pannexin channels acting as a conduit for at least some of the ATP efflux. To confirm a role of pannexins in this release, the effect of the pannexin blocking peptide ^{10}panx was examined. While 100 μM scrambled peptide (sequence FSVYWAQADR) had no effect on ATP release from swollen isolated neurons, addition of 100 μM ^{10}panx (sequence WRQAAFVDSY) substantially reduced the efflux of ATP (Fig. 2*G*).

To further explore the mechanism of release, inhibitors were added in combination. Addition of carbenoxelone with probenecid made no significant difference to the block produced by probenicid alone (Fig. 2*H*). Inclusion of the $P2X_7$ receptor antagonist A438079 with probenecid also had no additional effect on ATP release upon that observed with probenicid alone.

ATP release from stretched cells

While swelling induces mechanical deformation across the cell membrane, the magnitude of the deformation cannot be easily quantified and may induce additional strains. To examine the effect of a defined strain without cell swelling, cells were subjected to levels of mild stretch. Cells were attached to a silicone substrate in a specially designed chamber (Fig. 3*A*). As the design of the chamber precluded online measurement of ATP release, levels were measured from an aliquot of extracellular solution. The ATP obtained with this approach is more dilute and absolute levels of ATP are substantially lower, so the degradation of extracellular ATP by ectoATPases was inhibited by addition of ARL67156 and β,γ-methyleneATP ($\beta\gamma$mATP) to all solutions (Crack *et al.* 1995; Joseph *et al.* 2004). Application of 20 mmHg into the chamber led to a calculated strain of 4.1% (see Methods). While the magnitude of this pressure change is low, the degree of strain is in the range of that known to induce mechanosensitive responses in cells (Winston *et al.* 1989).

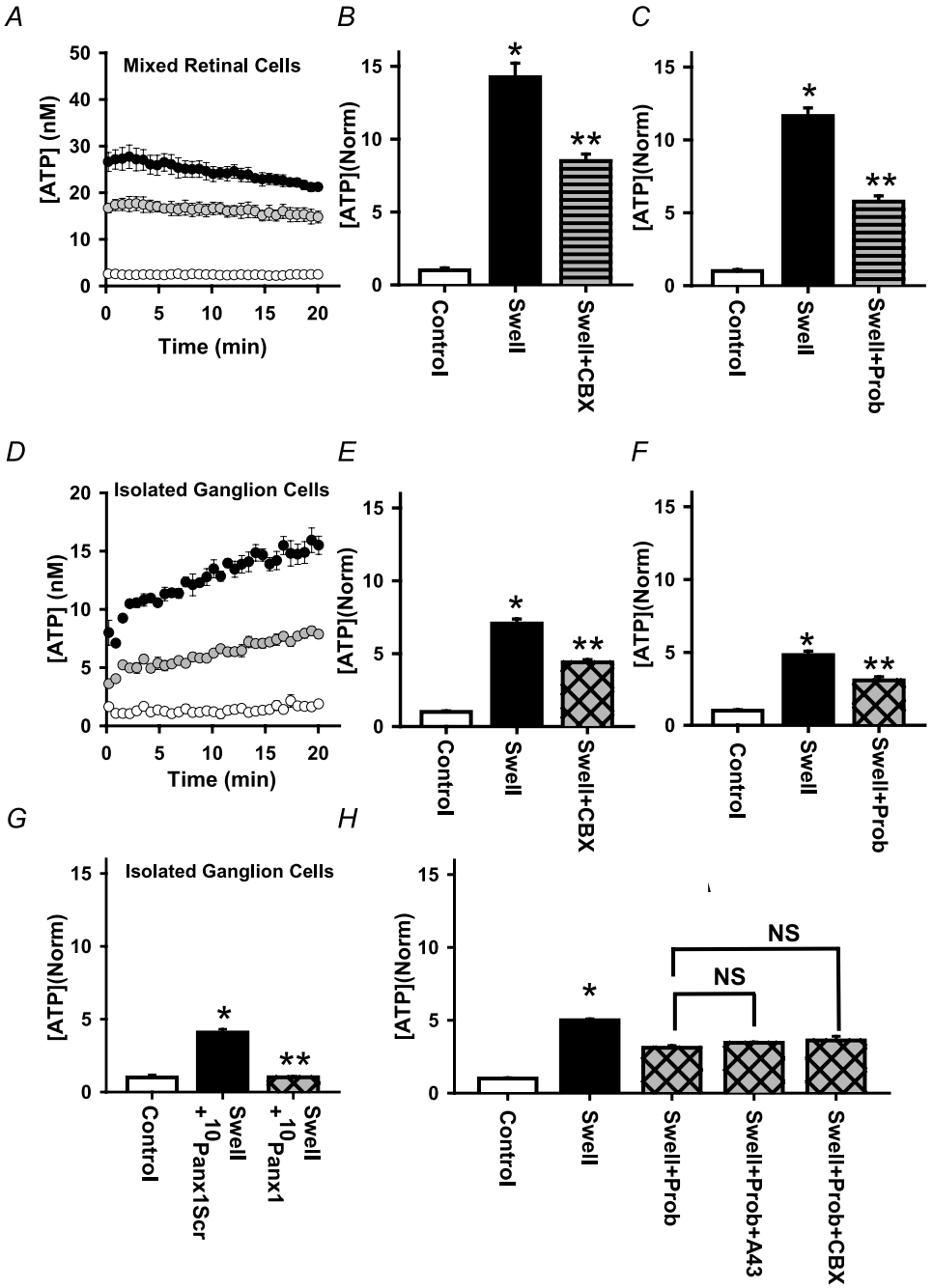

Figure 2. Swelling induced release of ATP from mixed retinal cells and isolated retinal ganglion cells involves pannexin channels

A, a representative curve portraying the ATP response from mixed retinal cells exposed to control isotonic solution (open circles), swollen in hypotonic solution (black circles) and hypotonic solution with 10 μM carbenoxolone (grey circles). *B*, swelling mixed retinal cells with hypotonic solution (Swell) led to enhanced release of ATP into the bath compared to cells bathed in control isotonic solution (Control). The presence of carbenoxolone (10 μM) inhibited the ATP response of cells in hypotonic solution (Swell +CBX; $n = 13$ for each; $^*P < 0.001$ *vs.* Control; $^{**}P < 0.001$ *vs.* Swell). *C*, the addition of 1 mM probenecid to the hypotonic solution also blocked the release of ATP from swollen cells (Swell + Prob; $n = 13$ for each; $^*P < 0.001$ *vs.* Control; $^{**}P < 0.001$ *vs.* Swell). *D*, a typical online measurement illustrating the ATP release kinetics from isolated retinal ganglion cells in response to control solution (open circles), swollen with hypotonic solution (black circles) and in hypotonic solution plus 10 μM carbenoxolone (grey circles). *E*, the mean response from isolated ganglion cells swollen by hypotonic solution (Swell) shows an increase in extracellular ATP concentrations as compared to isotonic control. Carbenoxolone (Swell+ CBX; 10 μM) inhibited this ATP response from isolated RGCs ($n = 20$ for each; $^*P < 0.001$ *vs.* control; $^{**}P < 0.001$ *vs.* swell). *F*, the swelling-induced release of ATP from isolated ganglion cells was also

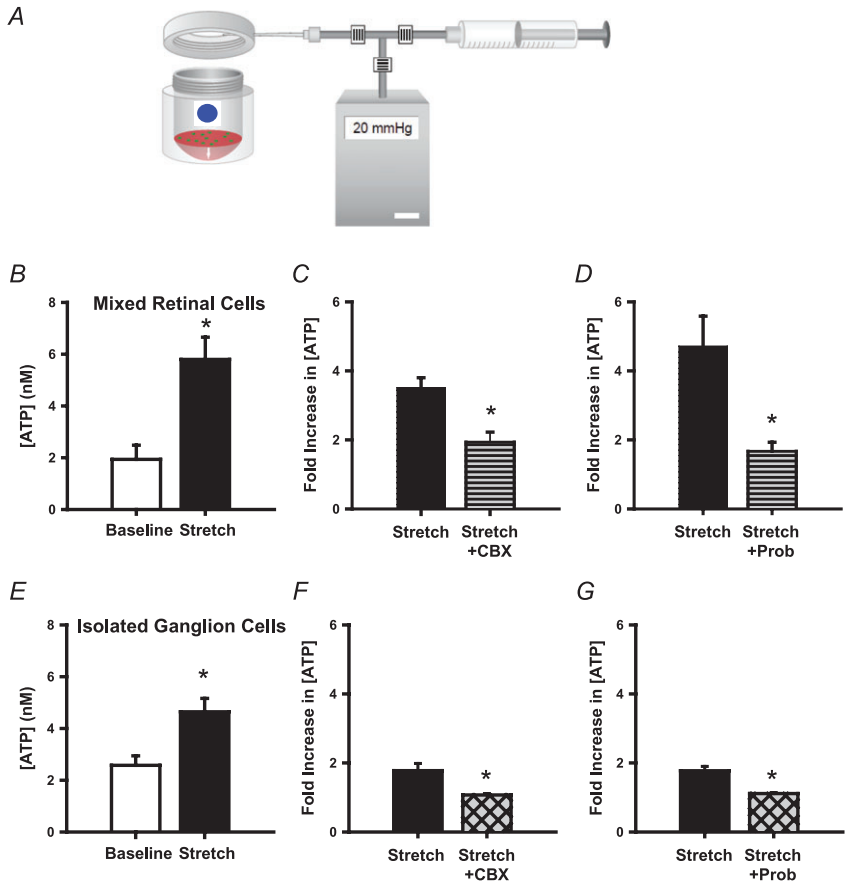

Figure 3. Stretching mixed retinal cells and isolated retinal ganglion cells leads to an increase in extracellular ATP through pannexin channels
A, schematic diagram of the specially designed stretch chamber used to stretch cells attached to an elastic silicone sheet. After careful washing with isotonic solution, a sample of the baseline ATP levels was collected at the location indicated by the dot and the top cover was screwed on with the appropriate precautions. Pressure inside the chamber was monitored with a digital manometer, as air was injected into the chamber from the syringe to increase pressure. Application of 20 mmHg of pressure led to a 4.1% deformation strain to the silicone sheet, thereby stretching the adherent cells. After stretching, the top enclosure was removed and a sample of the extracellular solution was collected at the same location. *B*, stretching mixed retinal cells led to increased extracellular ATP compared to baseline levels ($n = 4$, $^*P < 0.05$ *vs.* Baseline). For all experiments in this panel, ectoATPase inhibitors ARL67156 (100 μM) and β,γ-methyleneATP (100 μM) were added to the extracellular solution. *C*, carbenoxolone (CBX; 10 μM) significantly reduced the release of ATP in response to 20 mmHg of pressure from mixed retinal cells. Data are expressed as the extracellular ATP concentration after stretching normalized to baseline ATP levels to control for variation in cell density ($n = 5$ for each, $^*P < 0.05$ *vs.* Stretch alone). *D*, probenecid (Stretch+Prob; 1 mM) also inhibited the stretch-induced rise in ATP from mixed retinal cells ($n = 3$ for Stretch alone; $n = 4$ for Prob+Stretch; $^*P < 0.05$ *vs.* Stretch). *E*, isolated retinal ganglion cells also exhibited an increase in extracellular ATP levels when stretched ($n = 7$, $^*P < 0.05$ *vs.* Baseline). *F*, carbenoxolone significantly inhibited the release of ATP from isolated retinal ganglion cells exposed to stretch, as compared to pressure alone ($n = 10$ for stretch alone, $n = 12$ for stretch +CBX, $^*P < 0.05$ *vs.* stretch). *G*, probenecid (1 mM) also decreased the rise in ATP release from isolated retinal ganglion cells after stretch. ($n = 6$ for stretch; $n = 10$ for Probenecid (stretch + Prob); $^*P < 0.05$ *vs.* stretch alone.)

inhibited by probenecid (1 mM; Swell + Prob). $n = 20$ for each; $^*P < 0.001$ *vs.* control; $^{**}P < 0.001$ *vs.* hypotonic swell. *G*, the pannexin mimetic peptide ^{10}panx substantially reduced the swelling induced ATP release from isolated ganglion cells as compared to the scrambled control peptide (100 μM both, $n = 10$ for each; $^*P < 0.001$ *vs.* control, $^{**}P < 0.001$ *vs.* Swell + scrambled). *H*, the inhibition observed by adding 10 μM carbenoxelone and 1 mM probenicid to isolated ganglion cells was no greater than that observed with probenicid alone. Addition of the $P2X_7$ antagonist A438079 (10 μM) was also not additive. $n = 8$, $^*P < 0.05$ *vs.* control, $^{**}P < 0.05$ *vs.* swelling alone, NS – no significant difference, ANOVA on ranks.

The level of ATP in the bath surrounding mixed retinal cells was increased 3.62 ± 0.74-fold following stretch (Fig. 3*B*). Carbenoxolone (10 μM) blocked the release of ATP by stretching mixed retinal cells by $62.8 \pm 11.5\%$ (Fig. 3*C*) while probenecid (1 mM) inhibited $82.0 \pm 7.0\%$ of the ATP release from mixed retinal cells (Fig. 3*D*). While $\beta\gamma$mATP can activate P2X receptors in addition to blocking ectoATPase activity (North, 2002; Joseph *et al.* 2004), its presence in the bath of both control and swollen preparations suggests that any ATP release in Fig. 3 is due to the stretch and not activation of the P2X receptors, and thus its ability to increase ATP levels is due to its actions as an ATPase inhibitor.

Stretching the isolated neurons increased the extracellular level of ATP by 1.90 ± 0.19-fold (Fig. 3*E*). Again, the reduced magnitude is likely to reflect the decreased cell density of purified ganglion cells. Carbenoxolone inhibited the stretch-dependent release of ATP from purified ganglion cells by $90.9 \pm 5.6\%$ (Fig. 3*F*), whereas addition of 1 mM probenecid blocked the stretch-induced ATP release by $85.5 \pm 3.7\%$ (Fig. 3*G*). LDH levels in the bath were not significantly increased by stretching either mixed retinal cells ($P = 0.71$; $n = 4$) or isolated ganglion cells ($P = 0.69$; $n = 4$). This suggests that the ATP release induced by stretching was physiological and not due to cell lysis.

Swelling-activated currents in retinal ganglion cells

Although the luciferase experiments suggested that the application of mechanical strain to retinal ganglion cells led to the physiological release of ATP through pannexin channels, the functional effects of this release were unclear. Whole cell patch clamping was used to determine whether released ATP could autostimulate retinal ganglion cells. As the physical demands of the patch clamping technique precluded application of stretch to the cells, and as both swelling and stretching were shown to evoke a pannexin-associated release of ATP in Figs 1–3, mechanical strain was applied by swelling cells. Intracellular and extracellular solutions were chosen to isolate inward cation currents. To avoid activation of the voltage-dependent Na^+ channels, cells were kept at a holding potential of −60 mV and clamped from −60 mV to −100 mV in 5 mV steps (Fig. 4*A*). While baseline

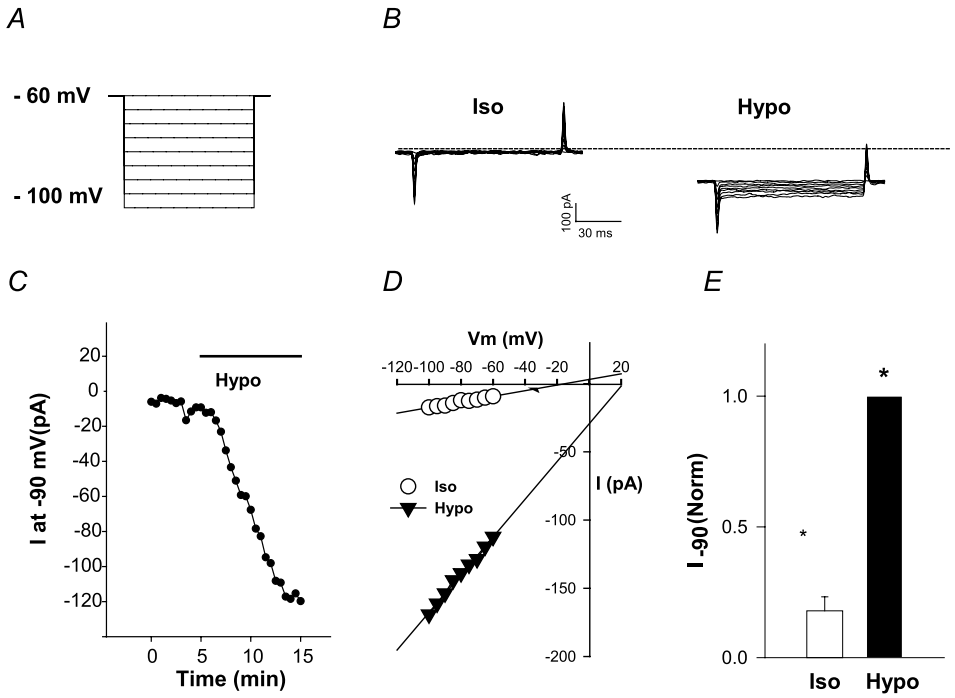

Figure 4. Cell swelling activates an inward cation current in retinal ganglion cells
A, voltage protocol used to characterize the currents activated by cell swelling. *B*, typical currents from ganglion cell in control isotonic solution (Iso) and swollen in hypotonic solution (Hypo). Fluorescently labelled ganglion cells were identified in a mixed cell population and patch clamped. Here and elsewhere, the dotted line indicates the zero level current. *C*, representative time course of swelling-activated current in retinal ganglion cells. Current observed at −90 mV (I at −90 mV) is shown for reasons of clarity. *D*, typical current–voltage curve indicating the substantial increase in inward current at physiological membrane potentials induced by cell swelling. The linear relationship implies that voltage-dependent Ca^{2+} or Na^+ channels were not activated at these potentials. *E*, overall, swelling retinal ganglion cells led to a significant increase in mean current at −90 mV (I_{-90}; $n = 4$, $^*P < 0.029$ *vs.* control). Here and throughout, currents were normalized to peak levels in hypotonicity.

currents were low, application of hypotonic solution led to the activation of a current in RGCs (Fig. 4*B*–*E*). The current was typically activated within 3–5 min (Fig. 4*C*), similar to the time course for ATP release. The reversal potential shifted to more depolarized potentials, consistent with an enhanced membrane permeability to Na^+ and Ca^{2+} (Fig. 4*D*).

Swelling-activated channels require autocrine stimulation of $P2X_7$ receptors by ATP

To determine whether the ATP released by ganglion cell deformation and the currents activated by ganglion cell swelling were causally related, the ability of antagonists to reduce the swelling-activated current was tested. Application of the soluble ecto-ATPase apyrase reduced the current activated by swelling (Fig. 5*A* and *B*). The current decreased by 1 U ml^{-1} apyrase showed linear kinetics over the 200 ms examined, with little sign of voltage dependence over the range tested (Fig. 5*C*). Baseline currents under control isotonic conditions were much smaller than the current blocked by apyrase, suggesting that the current observed after swelling the cell was dependent upon extracellular ATP. The reversal potential of the current in the presence of apyrase shifted back towards more hyperpolarized potentials, consistent with the removal of a current more permeable to Na^+, while the current–voltage relationship suggested the current behaved in an Ohmic fashion (Fig. 5*C*). Overall, the current at −90 mV was inhibited by 75 ± 7% ($n = 9$; Fig. 5*D*). This suggested that the swelling-activated current was largely dependent upon the presence of extracellular ATP.

As experiments above implied a mechanosensitive release of ATP through pannexin channels, the ability of pannexin channel antagonists to inhibit the swelling-activated current in ganglion cells was examined. Both 1 mM probenecid (Fig. 6*A* and *C*) and 10 μM carbenoxolone (Fig. 6*B* and *D*) reduced the swelling-activated current. The blocked currents displayed linear kinetics (Fig. 6*E* and *F*), while the blockers shifted the reversal potential back to more hyperpolarized potentials (Fig. 6*E* and *F*). Probenecid reduced currents at −90 mV by 60 ± 7% ($n = 10$; Fig. 6*G*), while carbenoxolone reduced the currents by 73 ± 11% ($n = 18$; Fig. 6*H*). The similarity between the currents inhibited by both carbenoxolone and probenecid suggests a role for pannexins in the response to swelling, although whether

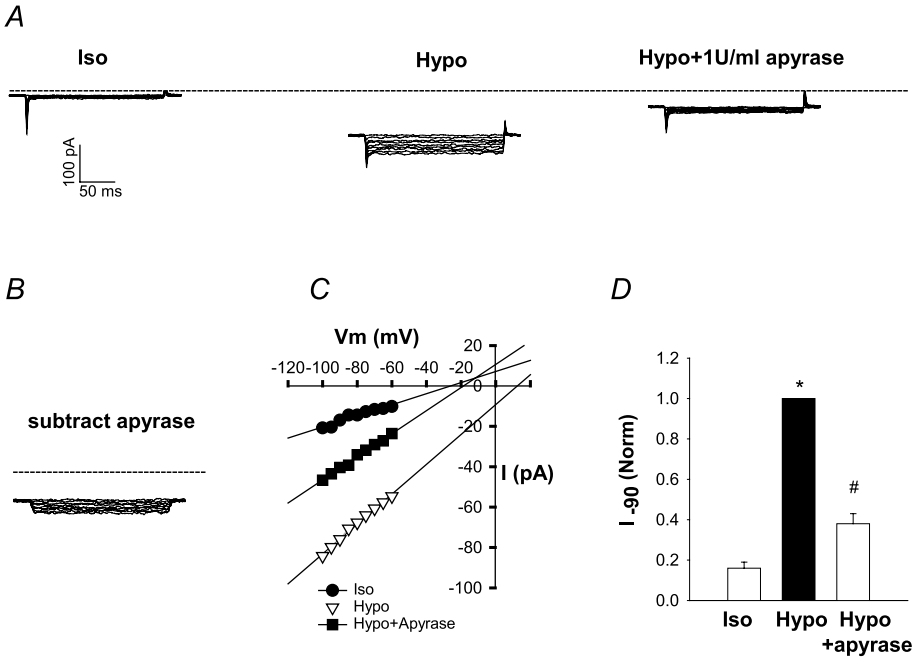

Figure 5. The current activated by swelling requires extracellular ATP
A, representative current recordings for a retinal ganglion cell exposed to control isotonic solution, hypotonic solution and hypotonic solution + 1 unit ml^{-1} of the soluble ATPase apyrase. Fluorescently labelled ganglion cells were identified in a mixed cell population. The dotted line indicates the zero level current. *B*, the net apyrase-inhibited currents at various voltages were obtained by subtracting currents found after apyrase application from those before. The lack of time-dependent inactivation or activation is evident. *C*, representative current–voltage plots in control, hypotonic solution, and hypotonic solution + apyrase indicate the Ohmic nature of the current. *D*, apyrase significantly inhibited currents activated by swelling cells ($n = 9$, $^*P < 0.05$ *vs.* Isotonic control; $\#P < 0.05$ *vs.* hypotonic alone). Currents were normalized to peak levels in hypotonicity.

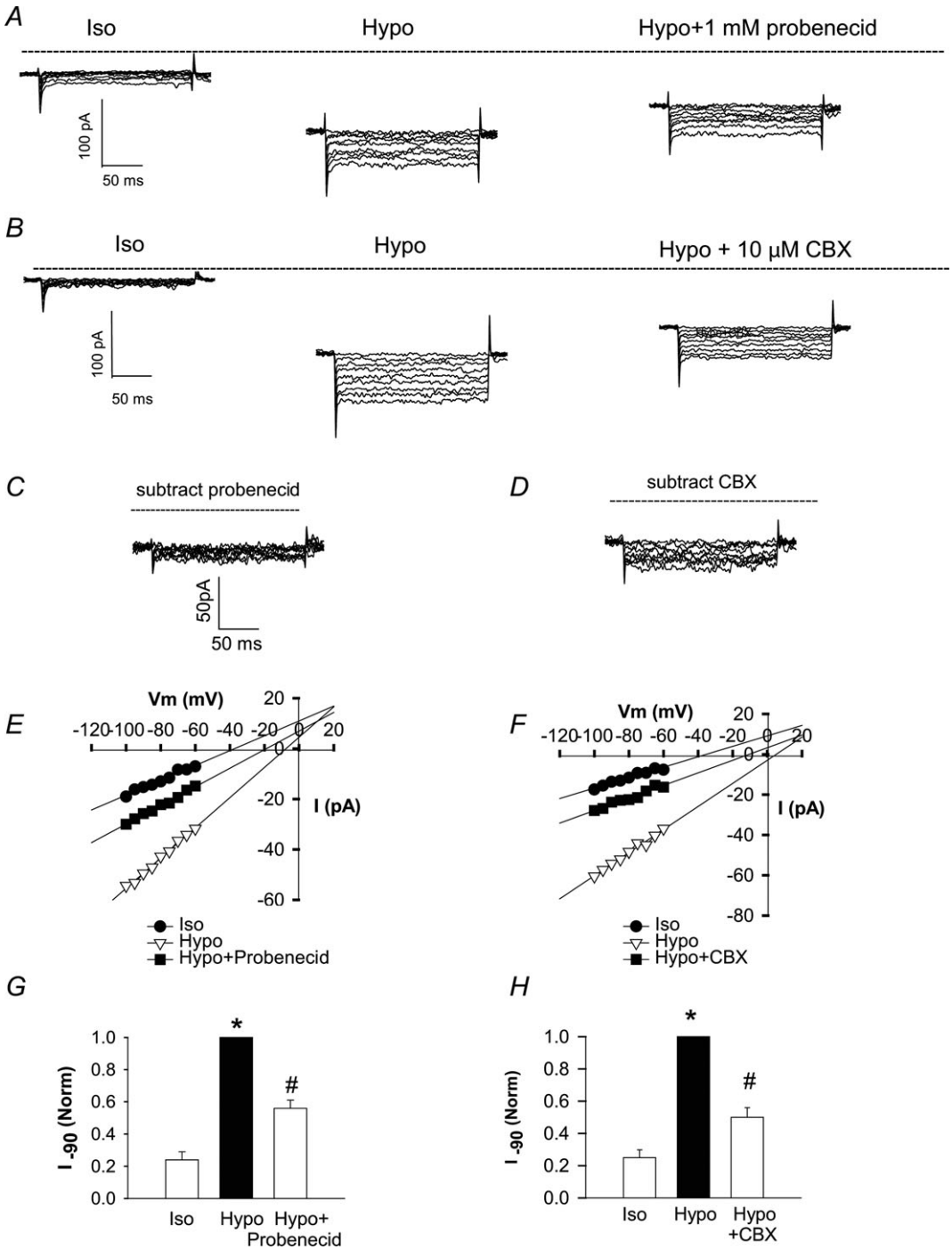

Figure 6. Pannexin hemichannel blockers probenecid and carbenoxolone inhibited whole cell currents activated by cell swelling in neurons

A and *B*, representative recordings of retinal ganglion cells in control isotonic solution, swollen in hypotonic solution, and swollen in the presence of hypotonic solution with 1 mM probenecid (*A*) or 10 μM carbenoxolone (*B*). Hypotonicity activated large inward currents that were blocked by pannexin hemichannel blockers probenecid or carbenoxolone. Fluorescently labelled ganglion cells were identified in a mixed cell population. The dotted line indicates the zero level current. *C* and *D*, the net probenecid and carbenoxolone-inhibited currents were obtained by subtracting the currents before from after application of probenecid (*C*) and carbenoxolone (*D*). *E* and *F*, representative current–voltage plots indicate the currents inhibited by probenecid (*E*) or carbenoxolone (CBX; *F*). *G* and *H*, probenecid (*G*) or carbenoxolone (*H*) produced a significant block of swelling-activated currents at −90 mV. $n = 10$ in *G*.; $n = 18$ in *H*. $^*P < 0.05$ compared to control isotonic, $\#P < 0.05$ compared to swelling in hypotonic solution alone. Currents were normalized to peak levels in hypotonicity.

the pannexin channel acts as a true mechanosensor or a downstream effector remains to be determined.

The ability of apyrase to inhibit the swelling-activated currents in ganglion cells also implied a role for extracellular ATP in the response. As these cells possess functional $P2X_7$ receptors (Zhang *et al.* 2005), $P2X_7$ receptor antagonists were added to test for a contribution from the receptor. At 1 μM, the $P2X_7$ receptor antagonist A438079 reduced the magnitude of the currents activated by cell swelling (Fig. 7*A* and *B*). The currents blocked by A438079 did not display time-dependent activation or inactivation, akin to those observed above (Fig. 7*C*). Blocking the $P2X_7$ receptor with A438079 shifted the reversal potential to more hyperpolarized potentials (Fig. 7*C*). Even at 1 μM, A438079 reduced the swelling-activated current by 75 ± 10% ($n = 9$; Fig. 7*D*).

The experiments in Figs 4–6 and 7*A–D* above were performed on ganglion cells present in mixed retinal cultures identified by the presence of fluorescent dye. While ganglion cells were typically located 30–100 μm

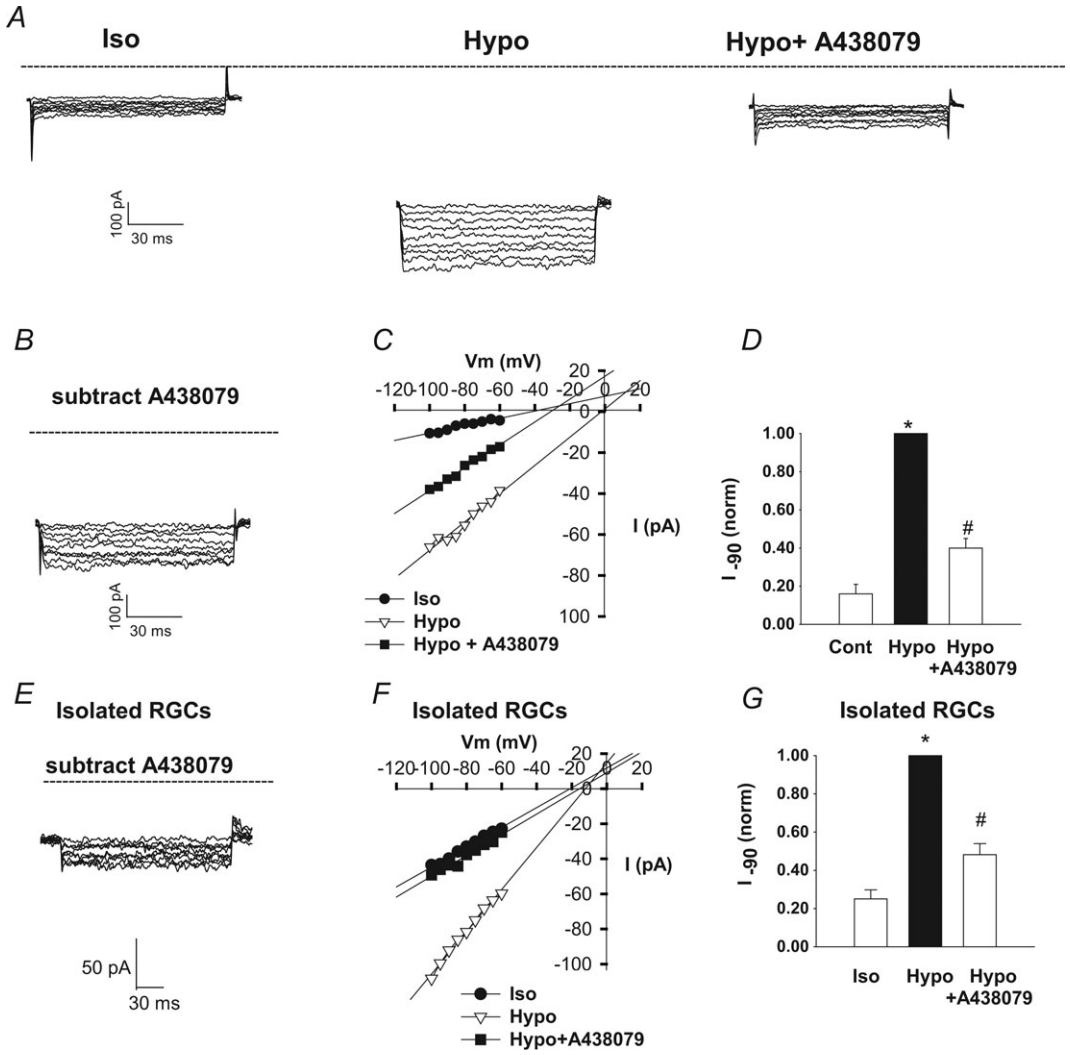

Figure 7. $P2X_7$ receptor antagonist A438079 inhibited whole cell currents activated by cell swelling from ganglion cells present in mixed retinal cultures and isolated immunopanned preparations *A*, typical whole-cell patch clamp recording from a ganglion cells in a mixed retinal cell preparation in control isotonic solution (Iso), swollen in response to hypotonic solution (Hypo), and swollen in the presence of $P2X_7$ receptor antagonist A438079 (Hypo + A438079; 1 μM). The dotted line indicates the zero level current. Currents were normalized to peak levels in hypotonicity. *B* and *C*, the currents blocked by A438079 were linear over time at all voltages tested (*B*, same scale as *A*), and displayed an Ohmic current–voltage relationship (*C*). *D*, A438079 significantly inhibited the swelling-activated currents at −90 mV ($n = 12$, $^*P < 0.05$ *vs.* Isotonic solution; $\#P < 0.05$ *vs.* hypotonic solution alone). *E* and *F*, whole cell recording of ganglion cells present in a preparation of purified immunopanned ganglion cells indicated that the swelling-activated currents inhibited by 1 μM A438079 were similar in terms of their linear kinetics (*E*), their Ohmic current voltage relations (*F*) and the proportion of current blocked (*G*; $n = 9$; $P < 0.05$ *vs.* isotonic solution; $\#P < 0.05$ *vs.* hypotonic solution swelling alone).

away from other cells, these experiments cannot definitively identify ganglion cells as the source of the released ATP. For this reason, whole cell recordings were performed on ganglion cells isolated by immunopanning. The swelling-activated currents in these cells were indistinguishable from those obtained previously. Critically, 1 μM A438079 blocked the swelling-activated currents in isolated cells (Fig. 7*E–G*). The current inhibited by A438079 displayed linear kinetics, increased Ohmically with voltage, and had a reversal potential implicating a Na^+ dominated cation permeability (Fig. 7*F*). The current in ganglion cells from isolated preparation was inhibited 74 ± 11% by 1 μM A438079 (Fig. 7*G*). This result is not significantly different from the response of ganglion cells present in mixed retinal cultures. The ganglion cells are thus themselves likely to be a source of mechanosensitive ATP release in these experiments.

While the block of the current by 1 μM A438079 was not complete, the drug has an IC_{50} of 400 nM at rat $P2Z_7$ receptors (Nelson *et al.* 2006). However, it also inhibits pannexin channels with an IC_{50} of ∼50 μM (Qiu & Dahl, 2009), complicating the interpretation of experiments using higher concentrations. To further confirm the contribution of the $P2X_7$ receptor to the swelling-activated current, additional experiments were performed. First, the actions of antagonist AZ 10606120 were examined. AZ 10606210 is a cooperative antagonist with an IC_{50} of 19 nM at rat $P2X_7$ receptors (Michel *et al.* 2008) and, to our knowledge, no known action on pannexin channels. Addition of 10 μM AZ 10606120 to swollen ganglion cells led to a rapid reduction in current that was voltage independent over the range tested (Fig. 8*A* and *B*). The antagonist inhibited the swelling-activated current at −90 mV by 85 ± 14% (Fig. 8*C*).

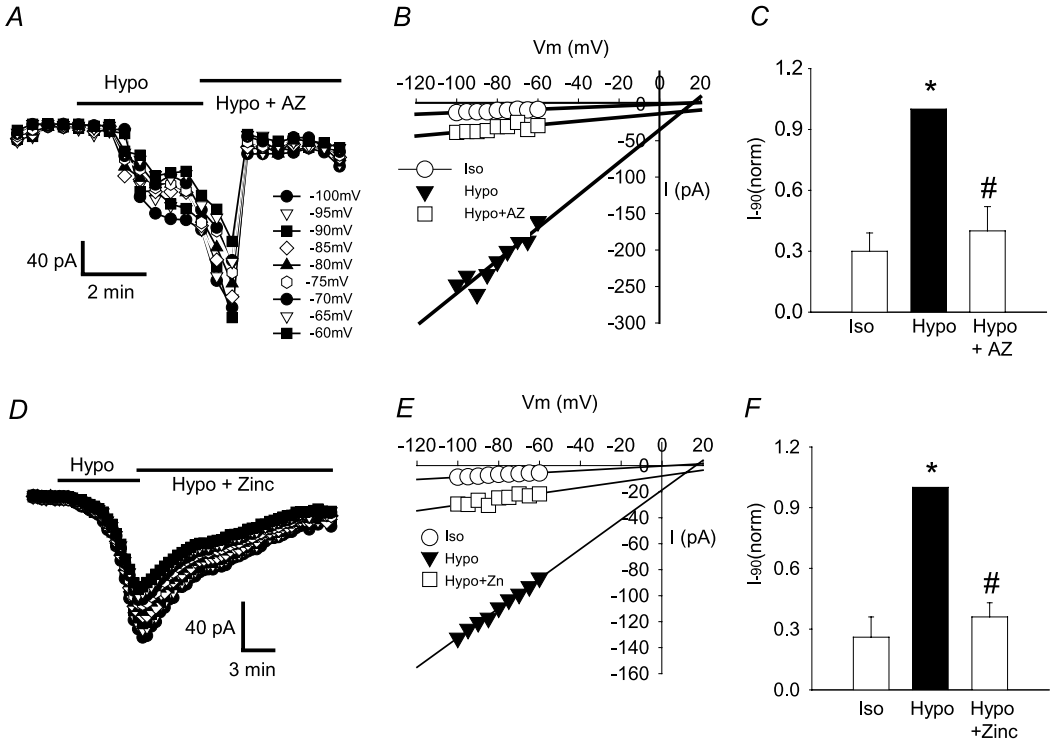

Figure 8. $P2X_7$ receptor antagonist AZ 10606120 and zinc inhibited whole cell currents activated by cell swelling in RGCs

A, representative traces of whole-cell patch clamp recording at different voltages in a fluorescently labelled ganglion cell from mixed retinal cell preparation in isotonic solution (Iso), following swelling in response to hypotonic solution (Hypo), and after the addition of 10 μM AZ10606120 to the hypotonic solution (Hypo + AZ). *B*, typical current–voltage curves in Iso, Hypo, and Hypo in the presence of AZ 10606120. The currents blocked by AZ10606120 were linear, and displayed an Ohmic current–voltage relationship. *C*, AZ10606120 significantly inhibited the swelling-activated currents at −90 mV by 85 ± 14% ($n = 4$, $^*P < 0.05$ *vs.* Iso; $\#P < 0.05$ *vs.* Hypo alone). The currents were normalized to peak levels in hypotonic solution. *D*, representative traces of whole-cell patch clamp recording at different voltages in a fluorescent ganglion cell from a mixed retinal cell preparation in isotonic solution, followed by swelling in hypotonic solution, and then swelling in the presence of 100 μM zinc (Hypo + Zinc). *E*, typical current–voltage curves in Iso, Hypo and Hypo in the presence of zinc. The currents blocked by zinc were linear, and displayed an Ohmic current–voltage relationship. *F*, zinc significantly inhibited the swelling-activated currents at −90 mV by 87 ± 4% ($n = 3$, $^*P < 0.05$ *vs.* Iso; $\#P < 0.05$ *vs.* Hypo alone). The currents were normalized to peak levels in hypotonic solution.

As a second test to specificity, the actions of Zn^{2+} were examined, as Zn^{2+} does not inhibit other P2X receptors, and actually enhances the current through some (North, 2002; Tittle & Hume, 2008). Zinc has a reported IC_{50} on the current through rat $P2X_7$ receptors of 11 μM (Virginio *et al.* 1997). Like AZ 10606120, application of 100 μM Zn^{2+} induced a voltage-independent block of the swelling-activated current (Fig. 8*D* and *E*). Zinc inhibited the swelling-activated current at −90 mV by 87 ± 4% (Fig. 8*E*). The blocks by AZ 10606120 and Zn^{2+}, when combined with the actions of A438079, strongly suggest that the $P2X_7$ receptor accounts for the majority of the currents detected in the swelling-activated current of retinal ganglion cells.

Influence of pannexins on RGC volume regulation

Additional experiments were designed to confirm the autocrine stimulation by testing if the swelling-induced release of ATP affected the ability of ganglion cells to regulate their volume. Isolated cells labelled with the brightly fluorescent dye calcein were exposed to hypotonic solution and the change in cell volume, as determined from the fluorescence, was recorded (Fig. 9*A*). The peak volume increased to 126 ± 4% of control when placed into hypotonic solution, but after 30 min in hypotonic solution cell size was reduced to 108 ± 1% of control, a regulatory volume decrease (RVD) of 78 ± 15% (Fig. 9*B*; $n = 9$), i.e. when cells were exposed to 1 mM probenecid and hypotonic solution together, the cells swelled to 127 ± 3% of control, but after 30 min this volume was decreased to only 118 ± 3% of control, a RVD of only 38 ± 8% ($n = 17$). This was significantly less than control, suggesting the release of ATP via pannexin channels contributes to the RVD in retinal ganglion cells.

Molecular and immunohistochemical identification of $P2X_7$ and pannexin-1 in isolated ganglion cells

Although the ability of pharmacological agents to inhibit ATP release and activation of the swelling current in ganglion cells provides important functional evidence for the involvement of $P2X_7$ and pannexin channels in ganglion cells, additional confirmation was sought at a molecular and protein level. Transcripts from *P2X*$_7$ or *panx1* genes were identified in isolated immunopanned

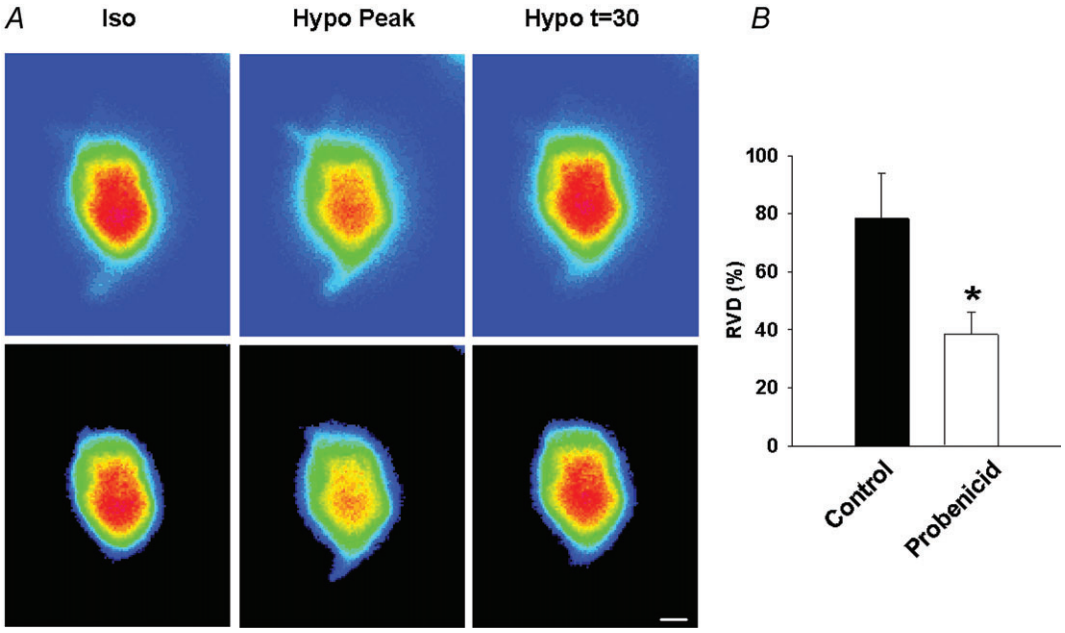

Figure 9. Pannexin hemichannel blocker probenecid inhibited regulatory volume decrease in isolated retinal ganglion cells
A, typical responses of isolated RGCs to hypotonicity. Images of RGCs loaded with fluorescent dye calcein in isotonic solution (Iso), hypotonic solution (Hypo Peak) and after 30 min in hypotonic solution (Hypo $t = 30$). The cell size was reduced from the peak after 30 min in hypotonic solution, indicating a regulatory volume decrease (RVD). Images are pseudocoloured for intensity; those at the top are raw images while those at the bottom display the cell area remaining after background was thresholded out, with remaining non-black pixels representing cell area. After conversion from area to volume, the volume in the centre (Hypo Peak) is 132% of control, and that at 'Hypo = 30' is only 115% of isotonic control. Scale bar = 10 μm. *B*, inhibition of RVD by probenecid. RVD was defined as the difference in cell volume at the swelling peak and 30 min after exposure to hypotonic solution (RVD (%) = 100 × (peak cell volume in Hypo – volume after 30 min in hypo)/(peak volume in Hypo – volume in Iso)). Probenecid (1 mM) significantly inhibited RVD. $n = 9$, control; $n = 17$, probenicid, $^*P < 0.05$ *vs.* control.

ganglion cells (Fig. 10*A*). Bands for the $P2X_7$ receptor were observed at the expected size of 392 bp. Interestingly, the *P2X7* band from the entire retina was less intense than from the isolated ganglion cells, suggesting the receptor transcripts were expressed at a higher concentration than in the retina as a whole. A band for *panx1* was identified at the appropriate size of 234 bp in brain, spleen, retina and isolated retinal ganglion cells. Sequencing of the transcript bands confirmed their identity.

Immunohistochemistry was used to determine the relative expression of $P2X_7$ and pannexin-1 channels. Isolated ganglion cells were grown for several days and cells showing neurite outgrowths were examined. Both $P2X_7$ and pannexin-1 were widely expressed on the soma and in the neurites (Fig. 10*B*). Close up inspection suggested that staining for the two antigens in the neurites was distinct.

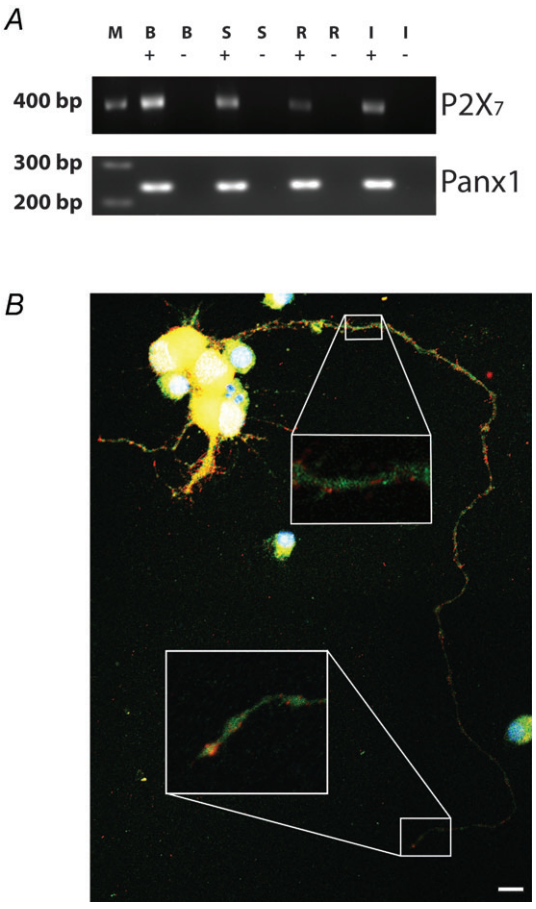

Figure 10. Molecular and immunohistochemical identification of the $P2X_7$ receptor and pannexin-1 in retinal ganglion cells
A, identification of bands from PCR using primers for *P2X7* (top) and *panx1* (bottom) mRNA. B: brain; S: spleen; R: whole retina; I: isolated ganglion cells. Molecular weight markers (M) are on the left. '+': reverse transcriptase included; '−': reverse transcriptase omitted. *B*, micrograph demonstrating pannexin-1 (green) and $P2X_7$ (red) staining in cultured retinal ganglion cell neurites. While neurites expressed both pannexin-1 and $P2X_7$, close-up inspection indicates the staining was distinct. While the soma expressed both antigens, the image is overexposed for somal staining in order to maximize detection in the neurites. Cell bodies are denoted by the nuclear stain DAPI (blue). Scale bar = 10 μm. Insets are 300% digital zooms of the areas of the axon marked by white squares.

Discussion

The data presented above strongly suggest that retinal ganglion cells are themselves capable of mechanosensitive ATP release and autocrine stimulation of $P2X_7$ receptors upon stretch. The pharmacological profile is consistent with pannexin channels as a conduit for this release, while the patch clamp experiments suggest that released ATP then autostimulates $P2X_7$ receptors on retinal ganglion cells. Together, they advance the novel hypothesis that neurons respond to mechanical deformation using autocrine purinergic signalling.

Several observations support the concept of mechanosensitive autostimulation. Firstly, ATP release was triggered by both swelling and stretching, with pannexin blockers inhibiting the ATP release from both forms of mechanical trigger to a similar extent (Figs 1–3). This implies that the release of ATP is a generalized response to mechanical strain in retinal ganglion cells. While neither probenecid, nor carbenoxolone nor the ^{10}panx peptide are specific for pannexins, a block by all three compounds at the concentrations used here strongly implicates pannexins as the conduit for ATP release. Carbenoxolone blocks less than 5% of the current through connexin hemichannels at 10 μM but inhibits pannexin-1 with an EC_{50} at 5 μM, while 1 mM probenecid blocks cloned pannexin-1 channels with no effect on connexin hemichannels (Bruzzone *et al.* 2005; Silverman *et al.* 2008). The permeability of pannexin-1 channels to ATP increased in response to membrane distension, identifying them as mechanosensitive conduits for ATP (Bao *et al.* 2004). The peptide ^{10}panx blocked the swelling-induced release of ATP; although the block was higher than that observed on ion currents, it has been suggested that the steric interference on movement of larger substances such as ATP may well be greater than for ions (Wang *et al.* 2007). Cumulatively, these results suggest a contribution from pannexin-1 in the mechanosensitive release of ATP from retinal ganglion cells, a role supported by the immunohistochemical identification of pannexin-1 in ganglion cells (Dvoriantchikova *et al.* 2006) and our identification of message for the *panx1* gene in isolated ganglion cells (Fig. 10).

Apyrase, probenecid, carbenoxolone, A438079, AZ 10606120 and zinc all inhibited swelling-activated currents with similar kinetic and voltage profiles (Figs 5–8). The ability of these drugs to target analogous currents suggests that the swelling-activated currents in retinal ganglion cells required functioning pannexin and $P2X_7$ receptors in the

presence of extracellular ATP. Several of the inhibitors can target multiple targets, such as zinc acting at P2Y receptors (Wildman *et al.* 2003) and A438079 acting at pannexin channels (Qiu & Dahl, 2009). However, the simplest explanation of the inhibition by all these antagonists is that swelling somehow opened pannexin channels to release ATP that then autostimulated $P2X_7$ receptors on ganglion cells. The various antagonists inhibited the current by 75–87%, and thus a minor contribution from additional P2 receptors insensitive to zinc cannot be completely ruled out. Probenicid blocked some, but not all, of the RVD or the current while a small current remained in the presence of apyrase. This suggests that an additional component exists that is not dependent on released ATP.

The detection of these currents in the absence of other retinal cell types supports this model (Fig. 7), and the parallel time courses for the swelling-induced current and the swelling-induced release of ATP from isolated ganglion cells reinforces the proposed relationship (Figs 1 and 4). Autocrine activation of purinergic receptors by ATP released after swelling has been observed in astrocytes and epithelial cells (Darby et *al.* 2003; Reigada & Mitchell, 2005). Autocrine activation of $P2X_7$ receptors occurs after ligation of CD3/CD28 in T cells (Yip *et al.* 2009), and the ATP released from neurons through pannexins in response to reduced glucose autostimulates A_1 adenosine receptors after conversion to adenosine by ectoATPases (Kawamura *et al.* 2010). The mechanosensitive autostimulation of neuronal $P2X_7$ receptors in ganglion cells demonstrated in the present study expands our understanding of autocrine neuronal signalling while also having implications for the management of neuronal diseases.

Pannexin-1 channels have been functionally associated with $P2X_7$ receptors, whereby the pannexins provide ATP at a sufficiently high concentration to activate the $P2X_7$ receptor (Qiu & Dahl, 2009). The considerable similarities in the pharmacological responses of the two receptor channels suggest an interdependence. This association may be relevant to retinal ganglion cells, as strong stimulation of the $P2X_7$ receptor can be lethal both *in vitro* (Zhang *et al.* 2005) and *in vivo* (Hu *et al.* 2010). The $P2X_7$ receptor requires ATP in high micromolar to low millimolar levels for activation (Surprenant *et al.* 1996), yet the abundance of local ectoATPases can greatly limit the available concentration of ATP, rapidly converting ATP released from adjacent glial cells into adenosine (Newman, 2001, 2003). Data presented here suggest that ATP released from mechanosensitive pannexin channels can autostimulate $P2X_7$ receptors, lending support to the concept of a functional $P2X_7$/pannexin unit on neurons. Given the dependence of $P2X_7R$ on high levels of ATP for activation, and given that ATP released from nearby glial cells is typically converted into adenosine before it reaches retinal ganglion cell membranes, the pannexin/$P2X_7$ unit would provide an ideal mechanism to overcome this limitation and supply a concentration of ATP capable of receptor stimulation.

Pannexin-1 channels expressed in oocytes displayed a maximum conductance of 475 pS, with several smaller subconductance states (Bao *et al.* 2004), but the whole cell conductance recordings in the current study did not display any large conductance steps. It is possible that the presence of mannitol, an inert sugar, partitions into the membrane to attenuate the pannexin channel currents, as has been shown for polyethylene glycols (Wang *et al.* 2007). It is also possible that pannexin-1 displays a lower conductance level in neurons. Recently, pannexins were strongly implicated in the neuronal response to amyloid β, even though stimulation triggered unitary events of only 30 pS (Orellana *et al.* 2011). Regardless of the reason for the reduced conductance, the ability of probenicid, carbenoxelone and the ^{10}panx peptide to inhibit ATP release strongly associate pannexins with the response in this study. The close similarities between the currents blocked by pannexin antagonists and $P2X_7$ receptor antagonists suggest that the current response is dominated by effects downstream of ATP release, although this remains to be confirmed.

Physiological implications

The demonstration that mechanical deformation activates autocrine stimulation of $P2X_7$ receptors on retinal ganglion cells has identified a potentially damaging signalling pathway for neurons. Acute elevation of intraocular pressure was elegantly shown to raise ATP and trigger blebbing of retinal ganglion cell neurites via $P2X_7$ receptors (Resta *et al.* 2007). The results presented here suggest that ganglion cells could themselves provide the injurious ATP during acute pressure elevations. Data in the current study demonstrates a role for ATP release in the RVD of swollen neurons (Fig. 9). While it is hard to predict the extent of neuronal swelling, these neurons are known to suffer from the mechanical strains associated with increased intraocular pressure. We have previously demonstrated that ATP is released in response to an acute rise in ocular pressure both *in vitro* (Reigada *et al.* 2008), and *in vivo* (Zhang *et al.* 2007) and have recently shown that ATP release accompanies chronic elevation in pressure (Li *et al.* 2011). Stimulation of the $P2X_7$ receptor kills retinal ganglion cells both *in vitro* (Zhang *et al.* 2005, 2006a) and *in vivo* (Hu *et al.* 2010). The contribution of this autocrine pathway to ganglion cells damage during chronic elevations in pressure would depend upon the cellular distribution of the proposed pannexin/$P2X_7$ receptor interactions, since structural analysis predicts that the laminar cribrosa responds most to this strain (Sigal & Ethier, 2009). While the spherical characteristics of the cells used in our patch clamp study suggests they

represent the ganglion cells somata, neurite projections from ganglion cells are replete with $P2X_7$ channels (Mitchell *et al.* 2009); the expression of both $P2X_7$ and pannexin channels on neurites in Fig. 10*B* suggests the ATP release/$P2X_7$ receptor autostimulation occur on the axons. Axons of dorsal root ganglion cells release ATP following an activity-dependent volume change, with this release acting to recruit glial cells for myelination (Fields & Ni, 2010). If the mechanosensitive autostimulation of $P2X_7$ receptors observed in retinal ganglion cells also occurs in cortical neurons, this may provide a new pathway by which mechanical strain or elevated pressure leads to pain or neuronal death. However, the recent demonstration that the $P2X_7$/pannexin system can be protective in acetylcholine-mediated seizures (Kim & Kang, 2011) suggests the interaction can also be beneficial.

References

Bao L, Locovei S & Dahl G (2004). Pannexin membrane channels are mechanosensitive conduits for ATP. *FEBS Letts* **572**, 65–68.

Barres BA, Silverstein BE, Corey DP & Chun LL (1988). Immunological, morphological, and electrophysiological variation among retinal ganglion cells purified by panning. *Neuron*, **1**, 791–803.

Beigi R, Kobatake E, Aizawa M & Dubyak GR (1999). Detection of local ATP release from activated platelets using cell surface-attached firefly luciferase. *Am J Physiol Cell Physiol* **276**, C267–278.

Boudreault F & Grygorczyk R (2004). Cell swelling-induced ATP release is tightly dependent on intracellular calcium elevations. *J Physiol* **561**, 499–513.

Bruzzone R, Barbe MT, Jakob NJ & Monyer H (2005). Pharmacological properties of homomeric and heteromeric pannexin hemichannels expressed in *Xenopus* oocytes. *J Neurochem* **92**, 1033–1043.

Burnstock G (1999). Release of vasoactive substances from endothelial cells by shear stress and purinergic mechanosensory transduction. *J Anat* **194**, 335–342.

Crack BE, Pollard CE, Beukers MW, Roberts SM, Hunt SF, Ingall AH, McKechnie KC, IJzerman AP & Leff P (1995). Pharmacological and biochemical analysis of FPL 67156, a novel, selective inhibitor of ecto-ATPase. *Br J Pharmacol* **114**, 475–481.

Darby M, Kuzmiski JB, Panenka W, Feighan D & MacVicar BA (2003). ATP released from astrocytes during swelling activates chloride channels. *J Neurophysiol* **89**, 1870–1877.

Drummond GB (2009). Reporting ethical matters in the Journal of Physiology: standards and advice. *J Physiol* **587**, 713–719.

Dvoriantchikova G, Ivanov D, Panchin Y & Shestopalov VI (2006). Expression of pannexin family of proteins in the retina. *FEBS Lett* **580**, 2178–2182.

Ferguson D, Kennedy I & Burton T (1997). ATP is released from rabbit urinary bladder epithelial cells by hydrostatic pressure changes–a possible sensory mechanism? *J Physiol* **505**, 503–511.

Fields RD & Ni Y (2010). Nonsynaptic communication through ATP release from volume-activated anion channels in axons. *Sci Signal* **3**, ra73.

Gonzalez-Sistal A, Reigada D, Puchal R, Gomez de Aranda I, Elias M, Marsal J & Solsona C (2007). Ionic dependence of the velocity of release of ATP from permeabilized cholinergic synaptic vesicles. *Neuroscience* **149**, 251–255.

Halassa MM, Fellin T & Haydon PG (2009). Tripartite synapses: roles for astrocytic purines in the control of synaptic physiology and behavior. *Neuropharmacology* **57**, 343–346.

Hu H, Lu W, Zhang M, Zhang X, Argall AJ, Patel S, Lee GE, Kim YC, Jacobson KA, Laties AM & Mitchell CH (2010). Stimulation of the P2X7 receptor kills rat retinal ganglion cells in vivo. *Exp Eye Res* **91**, 425–432.

Joseph SM, Buchakjian MR & Dubyak GR (2003). Colocalization of ATP release sites and ecto-ATPase activity at the extracellular surface of human astrocytes. *J Biol Chem* **278**, 23331–23342.

Joseph SM, Pifer MA, Przybylski RJ & Dubyak GR (2004). Methylene ATP analogs as modulators of extracellular ATP metabolism and accumulation. *Br J Pharmacol* **142**, 1002–1014.

Kawamura M Jr, Ruskin DN & Masino SA (2010). Metabolic autocrine regulation of neurons involves cooperation among pannexin hemichannels, adenosine receptors, and K_{ATP} channels. *J Neurosci* **30**, 3886–3895.

Kim JE & Kang TC (2011). The P2X7 receptor-pannexin-1 complex decreases muscarinic acetylcholine receptor-mediated seizure susceptibility in mice. *J Clin Invest* **121**, 2037–2047.

Kumar G, Kalita J & Misra UK (2009). Raised intracranial pressure in acute viral encephalitis. *Clin Neurol Neurosurg* **111**, 399–406.

Lau A, Arundine M, Sun HS, Jones M & Tymianski M (2006). Inhibition of caspase-mediated apoptosis by peroxynitrite in traumatic brain injury. *J Neurosci* **26**, 11540–11553.

Li A, Zhang X, Zheng D, Ge J, Laties AM & Mitchell CH (2011). Sustained elevation of extracellular ATP in aqueous humor from humans with primary chronic angle-closure glaucoma. *Exp Eye Res* **93**, 528–533.

Lim JC, Lu W, Eysteinsson T, Macarak EJ & Mitchell CH (2010). Mechanosensitive release of ATP from retinal ganglion cells through pannexin hemichannels. *Invest Ophthalmol Vis Sci*, ARVO E-Abstract 3308

Lossi L & Merighi A (2003). In vivo cellular and molecular mechanisms of neuronal apoptosis in the mammalian CNS. *Prog Neurobiol* **69**, 287–312.

Michel AD, Chambers LJ & Walter DS (2008). Negative and positive allosteric modulators of the $P2X_7$ receptor. *Br J Pharmacol* **153**, 737–750.

Mitchell CH, Fleischhauer JC, Stamer WD, Peterson-Yantorno K & Civan MM (2002). Human trabecular meshwork cell volume regulation. *Am J Physiol Cell Physiol* **283**, C315–326.

Mitchell CH, Lu W, Hu H, Zhang X, Reigada D & Zhang M (2009). The $P2X_7$ receptor in retinal ganglion cells: A neuronal model of pressure-induced damage and protection by a shifting purinergic balance. *Purinergic Signal* **5**, 241–249.

Mitchell CH, Lu W, Xia J, Lim J & Laties. AM (2010). Short-term effects of mechanical forces on retinal ganglion cells. *Exp. Eye Res.* ISER Abstract O130

Mitchell CH, Xia J, Lim J, Lu W & Laties. AM (2010a). Autocrine stimulation of neurons following mechanosensitive strain requires pannexin and P2X7 channels *Purines 2010*, P19-14 Abstract

Mitchell CH, Zhang JJ, Wang L & Jacob TJ (1997). Volume-sensitive chloride current in pigmented ciliary epithelial cells: role of phospholipases. *Am J Physiol Cell Physiol* **272**, C212–222.

Neary JT, Kang Y, Tran M & Feld J (2005). Traumatic injury activates protein kinase B/Akt in cultured astrocytes: role of extracellular ATP and P2 purinergic receptors. *J Neurotrauma* **22**, 491–500.

Nelson DW, Gregg RJ, Kort ME, Perez-Medrano A, Voight EA, Wang Y, Grayson G, Namovic MT, Donnelly-Roberts DL, Niforatos W, Honore P, Jarvis MF, Faltynek CR & Carroll WA (2006). Structure-activity relationship studies on a series of novel, substituted 1-benzyl-5-phenyltetrazole P2X7 antagonists. *J Med Chem* **49**, 3659–3666.

Newman EA (2001). Propagation of intercellular calcium waves in retinal astrocytes and Muller cells. *J Neurosci* **21**, 2215–2223.

Newman EA (2003). Glial cell inhibition of neurons by release of ATP. *J Neurosci* **23**, 1659–1666.

North RA (2002). Molecular physiology of P2X receptors. *Physiol Rev* **82**, 1013–1067.

Orellana JA, Shoji KF, Abudara V, Ezan P, Amigou E, Saez PJ, Jiang JX, Naus CC, Saez JC & Giaume C (2011). Amyloid β-induced death in neurons involves glial and neuronal hemichannels. *J Neurosci* **31**, 4962–4977.

Pascual O, Casper KB, Kubera C, Zhang J, Revilla-Sanchez R, Sul JY, Takano H, Moss SJ, McCarthy K & Haydon PG (2005). Astrocytic purinergic signaling coordinates synaptic networks. *Science* **310**, 113–116.

Qiu F & Dahl G (2009). A permeant regulating its permeation pore: inhibition of pannexin 1 channels by ATP. *Am J Physiol Cell Physiol* **296**, C250–255.

Reigada D, Lu W, Zhang M & Mitchell CH (2008). Elevated pressure triggers a physiological release of ATP from the retina: possible role for pannexin hemichannels. *Neuroscience* **157**, 396–404.

Reigada D & Mitchell CH (2005). Release of ATP from RPE cells involves both CFTR and vesicular transport. *Am J Physiol Cell Physiol* **288**, C132–C140.

Resta V, Novelli E, Vozzi G, Scarpa C, Caleo M, Ahluwalia A, Solini A, Santini E, Parisi V, Di Virgilio F & Galli-Resta L (2007). Acute retinal ganglion cell injury caused by intraocular pressure spikes is mediated by endogenous extracellular ATP. *Eur J Neurosci,* **25,** 2741–2754.

Sadananda P, Shang F, Liu L, Mansfield KJ & Burcher E (2009). Release of ATP from rat urinary bladder mucosa: role of acid, vanilloids and stretch. *Br J Pharmacol* **158**, 1655–1662.

Shitta-Bey AA & Neary JT (1998). Fluid shear stress stimulates release of ATP from astrocyte cultures. *FASEB J* **12**, A1469–A1469.

Sigal IA & Ethier CR (2009). Biomechanics of the optic nerve head. *Exp Eye Res* **88**, 799–807.

Silverman W, Locovei S & Dahl G (2008). Probenecid, a gout remedy, inhibits pannexin 1 channels. *Am J Physiol Cell Physiol* **295**, C761–767.

Surprenant A, Rassendren F, Kawashima E, North RA & Buell G (1996). The cytolytic P2Z receptor for extracellular ATP identified as a P2X receptor (P2X7). *Science* **272**, 735–738.

Tittle RK & Hume RI (2008). Opposite effects of zinc on human and rat P2X2 receptors. *J Neurosci* **28**, 11131–11140.

Treggiari MM, Schutz N, Yanez ND & Romand JA (2007). Role of intracranial pressure values and patterns in predicting outcome in traumatic brain injury: a systematic review. *Neurocrit Care* **6**, 104–112.

Virginio C, Church D, North RA & Surprenant A (1997). Effects of divalent cations, protons and calmidazolium at the rat P2X7 receptor. *Neuropharmacology* **36**, 1285–1294.

Wang J, Ma M, Locovei S, Keane RW & Dahl G (2007). Modulation of membrane channel currents by gap junction protein mimetic peptides: size matters. *Am J Physiol Cell Physiol* **293**, C1112–1119.

Wildman SS, Unwin RJ & King BF (2003). Extended pharmacological profiles of rat P2Y2 and rat P2Y4 receptors and their sensitivity to extracellular H^+ and Zn^{2+} ions. *Br J Pharmacol* **140**, 1177–1186.

Winston FK, Macarak EJ, Gorfien SF & Thibault LE (1989). A system to reproduce and quantify the biomechanical environment of the cell. *J Appl Physiol* **67**, 397–405.

Winters SL, Davis CW & Boucher RC (2007). Mechanosensitivity of mouse tracheal ciliary beat frequency: roles for Ca^{2+}, purinergic signaling, tonicity, and viscosity. *Am J Physiol Cell Physiol* **292**, L614–L624.

Woo K, Dutta AK, Patel V, Kresge C & Feranchak AP (2008). Fluid flow induces mechanosensitive ATP release, calcium signalling and Cl^- transport in biliary epithelial cells through a PKCzeta-dependent pathway. *J Physiol* **586**, 2779–2798.

Xia J, Lim JC, Lu W, Laties AM & Mitchell CH (2010). Mechanosensitive release of ATP via pannexins autostimulates P2X7 receptors on retinal ganglion cells. *Invest Ophthalmol Vis Sci* **51**, ARVO E-Abstract 3317.

Yip L, Woehrle T, Corriden R, Hirsh M, Chen Y, Inoue Y, Ferrari V, Insel PA & Junger WG (2009). Autocrine regulation of T-cell activation by ATP release and P2X7 receptors. *FASEB J* **23**, 1685–1693.

Zhang M, Budak MT, Lu W, Khurana TS, Zhang X, Laties AM & Mitchell CH (2006). Identification of the A3 adenosine receptor in rat retinal ganglion cells. *Mol Vis* **12**, 937–948.

Zhang X, Li A, Ge J, Reigada D, Laties AM & Mitchell CH (2007). Acute increase of intraocular pressure releases ATP into the anterior chamber. *Exp Eye Res* **85**, 637–643.

Zhang X, Zhang M, Laties AM & Mitchell CH (2005). Stimulation of P2X7 receptors elevates Ca^{2+} and kills retinal ganglion cells. *Invest Ophthalmol Vis Sci* **46**, 2183–2191.

Zhang X, Zhang M, Laties AM & Mitchell CH (2006a). Balance of purines may determine life or death of retinal ganglion cells as A3 adenosine receptors prevent loss following P2X7 receptor stimulation. *J Neurochem* **98**, 566–575.

Zhang Y, Phillips GJ, Li Q & Yeung ES (2008). Imaging localized astrocyte ATP release with firefly luciferase beads attached to the cell surface. *Anal Chem* **80**, 9316–9325.

Author contributions

All experiments were performed in Dr Mitchell's laboratory in the Department of Physiology and, after her move, the Department of Anatomy and Physiology with the exception of a few stretch experiments which were performed in Dr Macarak's laboratory. J.X.: collection, analysis and interpretation of data. J.C.L.: collection, analysis and interpretation of data. W.L.: collection, analysis and interpretation of data. J.M.B.: collection, analysis and interpretation of data. E.J.M.: conception and design of the experiments, drafting the article or revising it critically for important intellectual content. A.M.L.: conception and design of the experiments, drafting the article or revising it critically for important intellectual content. C.H.M.: conception and design of the experiments, drafting the article or revising it critically for important intellectual content. All authors gave approved of the final version of this manuscript.

Acknowledgements

This work is supported by grants from the NIH EY015537 and EY013434 (C.H.M.), EY017045 (A.M.L.), Vision Research Core Grant EY001583 (C.H.M. and A.M.L.), DK069898 (E.J.M.), Research to Prevent Blindness (A.M.L.), the Paul and Evanina Bell Mackall Foundation Trust (A.M.L.), and the Jody Sack Fund (W.L.). We would like to thank the Frank Stefano at the SDM Live Cell Imaging Core for assistance.